The diagnostics of thermal plasmas

D.C. Schram, J.A.M. van der Mullen, M.C.M. van de Sanden

Eindhoven University of Technology, Department of Physics, P.O. Box 513, 5600 MB Eindhoven, The Netherlands.

<u>Abstract</u> — Several diagnostic techniques and the underlying concepts are introduced at the hand of precision measurements in thermal stationary plasmas. The methods are illustrated with examples in slowly and strongly flowing plasmas.

1. INTRODUCTION

In the diagnostics of thermal plasmas the close to equilibrium state plays an important role [1]. This property and the relatively large electron density make a good precision reachable. But to specify the small deviations from local thermodynamic equilibrium such a good accuracy is also required.
For a first order description the LTE–assumption is usefull and often made. Together with one other parameter, as e.g. the pressure in isobaric conditions, it reduces the analysis of thermal plasmas to the determination of one quantity; usually the temperature, T. One can argue that the electron density n_e is a more characteristic quantity and easier to measure accurately [2].
On a more refined level even high density thermal plasmas in noble gases are slightly out of LTE in two respects. First the electron and heavy particle temperatures T_e and T_h may differ. Second the atomic level system may not be in full Saha equilibrium due to transport and radiation. In the literature several methods are presented to describe the non–equilibrium. In the "temperature approach" several temperatures are introduced (all of them indicating some non–equilibrium) [3]. In the "Boltzmann approach" the deviations of excited levels from Boltzmann equilibrium with the neutral ground state are used [4]. In this paper we will use the "Saha approach" [5] in which the deviation of the neutral ground state with respect to Saha equilibrium with the ion ground state is

used as the basic non–equilibrium parameter, $b_1 = n_1/n_1^s$. The reasons for this choice are threefold. First, it relates to directly measurable observables: densities; second Saha equilibrium starts at the higher excited levels and grows downward in the excited level energy space with increasing n_e; third, in many cases only the neutral ground state is out of Saha equilibrium. This case will be denoted by pLTE (as usual) except when also T_e and T_h differ; then it will be denoted here as pLSE [6]: partial local Saha equilibrium. To illustrate the methodology and to introduce several diagnostic techniques we will start with non flowing stationary cascade arcs which can be observed end on and allow for a good accuracy.

2. END ON OBSERVED STATIONARY PLASMAS

The first optical technique to be discussed is the absolute line intensity method. If the line is optically thin, the absolute emissivity, ϵ_{ul} is proportional to the upper state level density n_u which in pLSE is equal to the Saha density:

$$\epsilon_{ul} = n_u \ A_{ul} h \nu_{ul}/4\pi; n_u/g_u = n_u^s/g_u = \frac{n_e}{g_e} \frac{n+}{g+} (\frac{h^2}{2\pi m_e k T_e})^{3/2} \exp(E_p^{ion}/kT_e) \tag{1}$$

If several lines with different upper levels are measured a Saha–Boltzmann plot (fig. 1) can be constructed, the slope of which gives T_e and the absolute value gives n_e. However, the accuracy needed to conclude a deviation from equilibrium can hardly be reached as the transition probabilities A_{ul} are usually not known with the required precision and small but finite deviations from equilibrium even for excited states in particular in the lower n_e range ($n_e \sim 10^{21} - 10^{22}/m^3$) will occur. In pLTE n_e (or T_e) can be deduced with reasonable accuracy from one absolute line intensity, if the plasma is close enough to LTE. Two quantities of the three (n_e, T_e, b_1) are needed to describe

a pLTE if the pressure, p, is known. If one assumes a value for b_1 (including the $b_1=1$, LTE) one can relate the density of a state to either n_e or T_e; b_1 is then a parameter. In fig. 1^b the 5^d–density of Ar I is shown as a function of T_e for three values of b_1 (0.1, 1, 10) from [2] [7]. It is clear that within this b_1–range the uncertainty in the T_e determination is only 10%; for n_e it is even better. This absolute line intensity method works also for the pLSE situation; then b_1 has to be replaced by $b_1 T_h / T_e$ in the reasoning above.
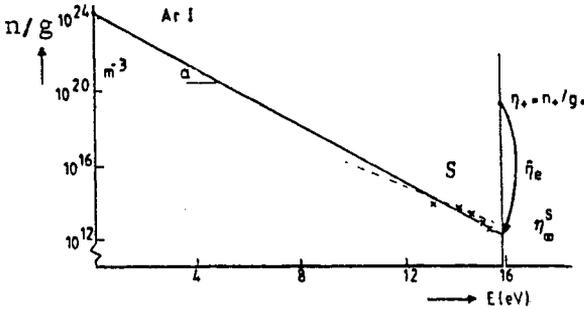

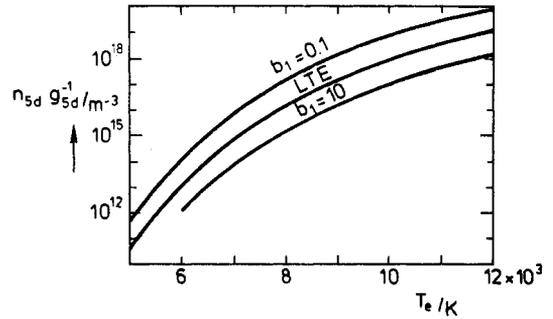Fig. 1^a. Saha Boltzmann plot for ICP parameter

Fig. 1^b. The relation between n_{5d}/g_{5d} and T_e with b_1 as parameter g_{5d} [2]

In the more refined source function method a partially absorbed line is observed both without (I_1) and with (I_2) a reflected signal from a parabolic mirror at the other side. This measurement is performed as a function of wavelength. In the Stark shifted line centre the absorption makes the two intensities nearly equal. In the wings of the line the plasma is transparent and I_2 is equal to $I_1 (1 + \tau^2 R \exp[-\kappa l]) I_1$, i.e. the same intensity I_1 plus a from the other side reflected and again partially absorbed signal ($\tau^2 R$ accounts for window transmission and mirror reflection losses).
The intensity I_1 can be related to the emissivity and absorption coefficient: $I_1 = (\epsilon_\lambda (1 - \exp[-\kappa l])$. In pLSE ϵ_λ and κ_λ are related to the source function

$$S_\lambda = \epsilon_\lambda / \kappa_\lambda = 2hc^2 \lambda^{-5} (\exp^{hc}/\lambda k T_e - 1)^{-1} \qquad (2)$$

By measuring the λ–dependences of I_1 and I_2 (absolutely) the value for T_e can be determined without any knowledge of the transition probability. The integrated value of $\kappa_\lambda d\lambda$ gives the lower state density if the transition probability is known and a proper correction for the continuum is performed. This method has been used [5] to establish the non–equilibrium relation between n_e and $T_e = T$ for argon at 1 atmosphere (fig. 2). It is observed that at given T the pLTE value of n_e is somewhat lower than the LTE value. This is to be expected for an ionizing system as the ground state of neutrals is somewhat overpopulated to take care of ionization to compensate diffusive and radiation losses. The precision of the source function method is better than the absolute line intensity method. Calibration errors give errors in n_e and T such that the error bar is parallel to the pLTE curve; hence the accuracy of the non–equilibrium (~ 1%) is better than the accuracy of n_e (2%) and T (5%) seperately. A very high accuracy in T_e can be reached if one starts from a n_e measurement, which is independent on LTE assumptions, like interferometry. From this n_e value (4% error) a T (LTE) and, if the pLTE relation is known also the actual T (pLTE) can be obtained from the LTE or pLTE relations at given pressure. From figure 2 it can also be deduced that n_e is usually a better thermodynamic variable than T; therefore it is appropriate to focus now on n_e–measurements as interferometry, continuum analysis and Stark broadening.
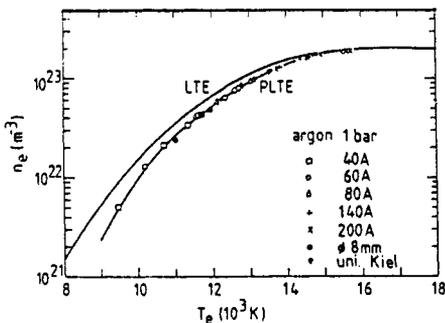

Fig. 2^a. The LTE and pLTE relations between n_e and T_e [5]
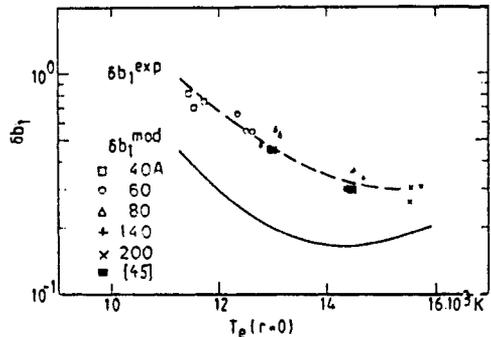
Fig. 2^b. The resulting non–equilibrium parameter b_1 as function of T_e [5]

<u>Interferometry</u>: at the high electron and neutral densities of thermal arcs a combination of visible and IR sources is optimum. The IR (λ_2=3.39 μm) probes primarily the electrons, the visible (λ_1= .633 μm) the neutrals and ions [4],[8]. With the two interferometers (in [5] of the coupled cavity type) the phase shifts are measured. Expressed in the so—called fringes $\Delta(\lambda_{1,2})$ (2π optical path length phase changes) the electron density and neutral density times interaction length are equal to [5]:
$$n_e L = -3.404 \ 10^{20} \ \Delta(\lambda_2) + .628 \ 10^{20} \ \Delta(\lambda_1)$$
$$n_0 L = -.558 \ 10^{22} \ \Delta(\lambda_2) + 3.099 \ 10^{22} \ \Delta(\lambda_1)$$
The precision obtainable with the two λ—interferometry is very high. Interlaboratory comparison has been made [9] and the conclusion is that 2–3% accuracy is obtainable, if the inaccuracy in the arc length is avoided by taking two arc lengths.
To measure n_e at lower densities longer wavelengths must be used: CO_2 laser or Far Infrared Lasers (FIR). The latter are abundantly used in fusion research [10] but not so much in atomic plasmas.

<u>Continuum emission</u> has three contributions in atomic gases: free free from electron neutral scattering ϵ_{ff}^{eo}, free free from electron—ion scattering, ϵ_{ff}^{ei} free—bound from radiative recombination ϵ_{fb}. For several gases (in particular argon) the corresponding ff and fb factors have been determined. For ionization degrees above a few percent, absolute measurement of the continuum emission in the visible provides an accurate way to determine the electron density. By measuring the emissivity also in the UV the electron temperature can be determined as well. The fb factor for Ar I is summarized by e.g. Wilbers et al. [11].
In the regime of high ionization degree ($n_e/n_0 > 1\%$) the ff^{eo} contribution can be neglected; as the ff^{ei} and the fb contributions are proportional to n_e^2 and only weakly dependent on T_e (in the visible) the continuum emission gives n_e directly, independent of assumptions on equilibrium. If ff e—o emission plays a significant role, the value of n_0 must be known and an additional non—equilibrium parameter is needed in pLTE [11],[12].

<u>Stark broadening</u> and shifts can be measured if the wavelength resolution is sufficient. (In the source function method this is anyway required). At higher electron densities the Lorentzian Stark broadening exceeds the Gaussian Doppler broadening. By fitting techniques from the Voigt emissivity profile the Lorentz and Gauss components can be extracted. After correction for the apparatus profile, the Stark width and shift can be determined. In the range $n_e > 10^{21}/m^3$, this gives a possibility to determine n_e from e.g. Ar I broadening. A typical broadening for Ar I lines is a few tenths of a nm for $n_e = 10^{23}/m^3$ and $T_e = 15000$ K [13]. Argon—ion line broadenings are smaller (e.g. 0.17 nm at $n_e = 10^{23}/m^3$ for the Ar II 442.6 nm line [14]. The accuracy is limited due to two factors. First in the simulation there is a strong coupling between continuum and Lorentzian wings of the line. Second, accurate experimental Stark parameters are not always available. Still Stark broadening is very useful as it is relatively simple. This is even more true for the hydrogen Balmer lines. Hydrogen exhibits a linear Stark effect and at higher densities the widths and shifts are very large. But also at lower densities of $10^{21}/m^3$ they are readily measured. The $n_e^{2/3}$—dependence for high n_e turns into a n_e^1 dependence at lower n_e as has been shown by Helbig [15]. In a critical review he indicates a preference for the Hβ for high density regime and for the Hα for lower n_e.
In this section we treated end on observed optical diagnostics of axially homogeneous stationary systems. In the following we will treat flowing systems, a situation prevalent in plasma chemical applications. These systems have to be observed side on and to reach precision Abel inversion is needed. First we will treat a relatively slowly flowing system: the ICP.

3. SLOWLY FLOWING SYSTEMS; THE INDUCTIVE COUPLED PLASMAS (ICP)

To investigate the non—equilibrium state of an ICP (fig. 3^a) as used in spectrochemistry, cf. [16] [17] first pure argon plasmas have been studied by absolute line intensity method. The laterally observed line intensities were Abel inverted; some of the observed profiles are hollow and care is needed to reach sufficient precision. The thus obtained radial profiles are analysed using the close to equilibrium concepts described in section 2. Results in terms of radial profiles for assumed $b_1 = 10; 1; .1$ are displayed in fig. 3^b [18]. In this figure also Balmer Hβ broadening results are shown. Stark broadening is a very good way for determination of n_e by sidewards observation. With Abel inversion of the full profile at any wavelength, radial λ profiles can be determined and with that a radial n_e profile [18].
We conclude that the absolute line intensity method gives already satisfactory results for $0.1 < b_1 < 10$. But on a more refined level we see also that the differences between the Hβ method and the absolute line intensity method can give information on the non—equilibrium (on b_1).

Extremely powerful is the experimental technique of following the response to the RF—power interruption for various line intensities. This technique initially introduced for arc plasmas [19],[8] has been applied by Fey et al. [20] to ICP's. They observe a direct, instanteneous response discussed here and a delayed response discussed by Stoffels et al. at this conference.
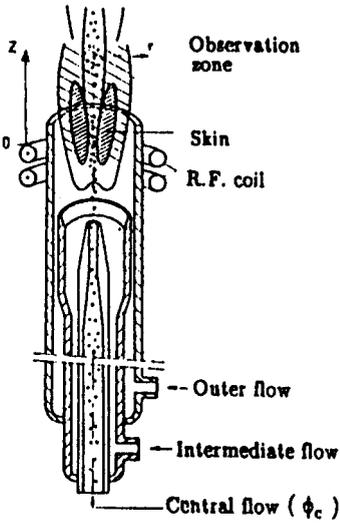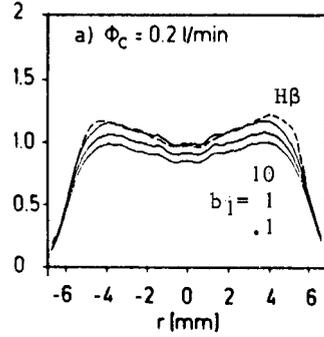
Fig. 3ᵃ. A sketch of an ICP

Fig. 3ᵇ. Density measurements as measured by absolute line intensity method and by Hβ–broadening [18]

The instanteneous responses are based on the interruption of the energy balance. Schematically the electrons {e}, heated by the RF field, lose energy in collisions with heavy particles {h} which in their turn are cooled by convection and conduction. As a consequence $\gamma = T_e/T_h > 1$ in the steady state. Interrupting this E–balance will initiate two decay phenomena of the electron gas {e} with two different timescales; i.e. the relaxation of energy (T_e with $\tau_e \simeq 1$ μs) and of density (n_e with $\tau_n \simeq 1$ ms). Therefore the disturbance effected by the power interruption causes at each location a series of instantaneous events:

1) Cooling; after the switch off the electrons cool down form T_e to $T_e^* = T_h$ (with $\tau \simeq \tau_e$)
2) Recombination; n_e decreases "slowly" with a time constant τ_n.
3) Heating; the reverse of cooling at switch on; a sudden increase of T_e in ($\tau \approx \tau_e$)
4) Ionization: a slow increase during $\tau \simeq \tau_n$ of the density to its original value.

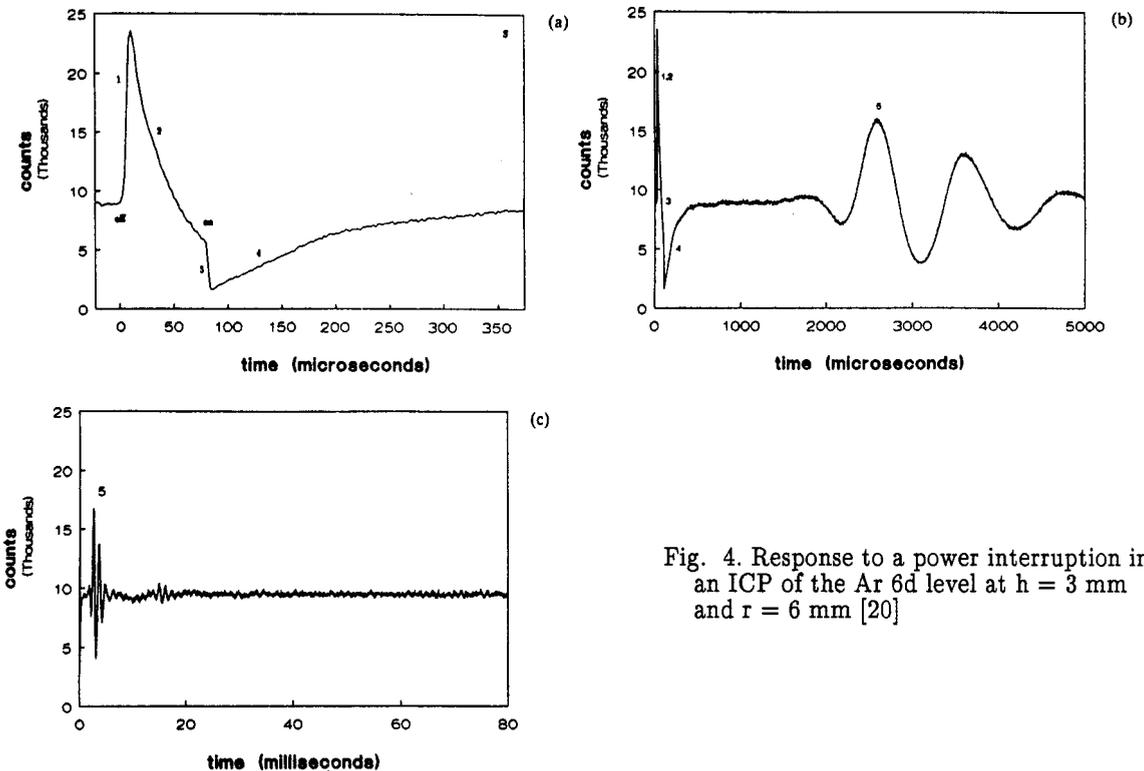

Fig. 4. Response to a power interruption in an ICP of the Ar 6d level at h = 3 mm and r = 6 mm [20]

In fig. 4 showing the response of an Ar line the events 1–4 are depicted. For Ar levels the intensity jumps upwards at cooling; at heating the jump is downwards. The response of the line intensity can be traced back to production/destruction balances of the relevant levels. For Ar levels a Saha–like response is observed; highly excited Ar states are expected to be in pLSE, i.e. determined by the Saha balance (cf. eq. (1)) which equilibrates rapidly (within $\tau_s \ll 1\ \mu s$). So, eq. (1) can be employed at any time, provided the appropriate values of n_e and T_e are substituted. The value of the cooling jump can be obtained using eq.(1) for T_e and T_h respectively which gives the ratio of densities before (n_p) and after (n_p^*) cooling. In logarithmic form:

$$\ln \frac{n_p^{s*}}{n_p^s} = \frac{\gamma - 1}{kT_e} I_p^{ion} + \frac{3}{2} \ln \gamma \qquad \text{'Saha'} \ ; \gamma = T_e/T_h \tag{3}$$

The derivations are based on the assumption that n_1, n_e and n_+ are constant during cooling. Plotting the measured height of the cooling jump of Ar levels as a function of I_p^{ion} (ionization energy of level p) should give a straight line from which T_e and T_h can be deduced (cf. eq.(3)). This procedure [4], [20],[21] must be done with spatially resolved values for both n_p and n_p^*. Assuming that lateral measurements of the skin give spatially resolved information, this method yields values for T_e/T_h and T_e [20].

The same procedure can also be used to get information on the electron temperature T_e^{**} immediately after switching on the generator. From the large heating jumps we can conclude [20] that this T_e^{**} value is much higher than the steady state value. This study once more clarifies that it useful to distinguish between the departure of LTE as created by the inequality $T_e \neq T_h$ and the departure from the Saha equilbrium which is level dependent. Note, that in the present derivation only the observed excited level needs to be in Saha equilibrium (and not all excited levels).

The delayed response is caused by a disturbance created during the power interruption and frozen in the flow. By plotting the time of arrival of the ringing as a function of position a linear behavior is found corresponding [20] to a velocity of 12 m/s. It is an example of flow measurements by following optically a disturbance.

4. STRONGLY FLOWING PLASMAS AND EXPANDING PLASMAS

In this section spectroscopic methods on systems with systematic velocities approaching the thermal velocity are described. Here we refer to spraying plasmas and (lower pressure) expanding cascade arc plasmas. The flow is similar as in the ICP case (100 scc/s), but the channel cross section is smaller and hence the velocity higher. As a consequence there are no isobaric conditions and the pressure must be measured in particular for the expanding cascade arc case. First we will treat methods used on spraying plasmas. These plasmas are observed in the plume with full access for lateral observation. T_e has been measured [22] using the Ar II line continuum ratio. In the optically thin case the Ar II line intensity is proportional to $n_e.\exp[-E_p/kT_e]$ in which E_p is the excitation energy.

The continuum intensity is proportional to n_e^2. By assuming the Ar II underpopulation factor $a_p^{II} \simeq 1$ and by taking the (p = 1 at.) pLTE n_e, T_e curve of fig. 2, T_e can be obtained from the line continuum ratio. In fig. 5 the resulting T_e profile is shown together with a n_e profile from H–β Stark broadening. We note that it would be possible to use also an Ar I line continuum ratio. The Ar I levels will be in Saha equilibrium and vary according to $n_e^2 g(T_e)$. Therefore, the ratio gives directly T_e independent of the non–equilibrium of lower levels.
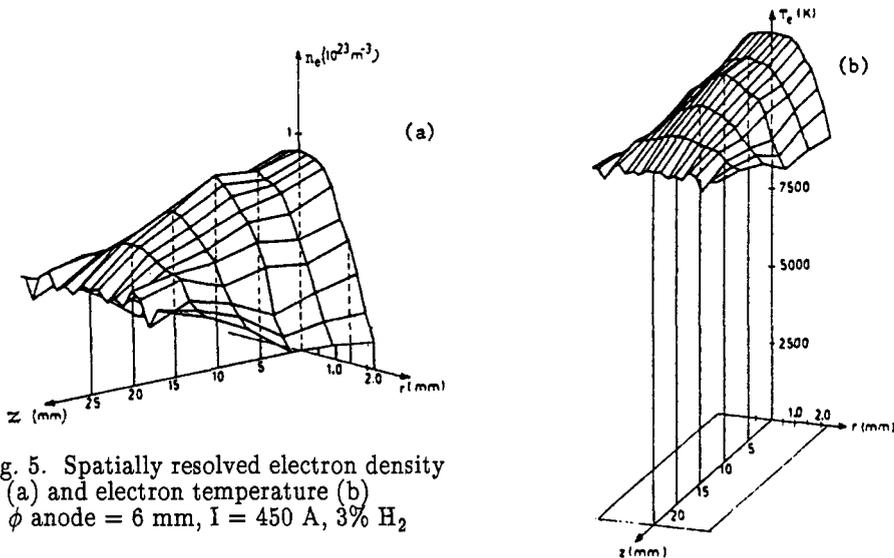

Fig. 5. Spatially resolved electron density (a) and electron temperature (b) ϕ anode = 6 mm, I = 450 A, 3% H_2

A second subject is the measurement of velocities. One method is to introduce axially very small particles (a few μm) in the flowing plasma; the velocity is then measured by a (dual beam) laser Doppler anemometer. Results obtained this way by Vaessen [22] are shown in fig. 6. The first increase in velocity is due to finite slip between plasma flow and test particles. A new method is to cross correlate fluctuations frozen in the flow, observed at two positions in the plasma flow; the flow velocity can be determined from the time difference for maximum correlation. Refined techniques have also been developped to measure in flight the temperature of the spray–particles. For these methods [1] we refer to papers given by Fauchais et al. and by Vardelle et al. at this conference.
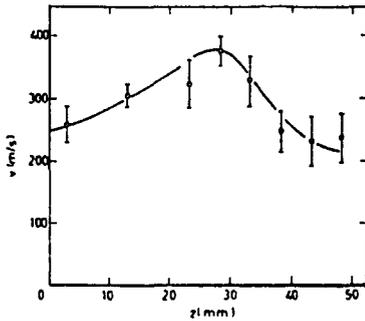

Fig. 6. Velocity measurement of a plasma spraying plasma [22]
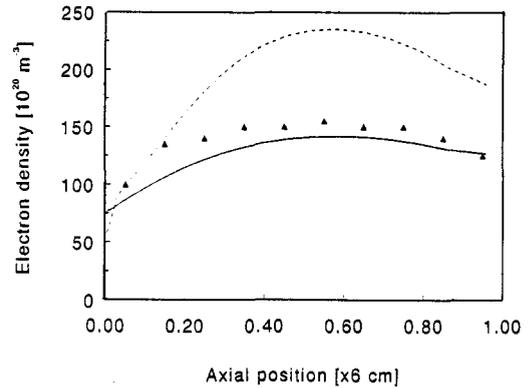

Axial position [x6 cm]

Fig. 7. Meausured (.) and calculated electron densities (dashed line, peak value, full line: average value) [25]

Let us now turn to the expanding cascade arc used for high rate plasma deposition [23]. In these experiments a flush wall in the cascade arc source section is very important; hence lateral scanning is there impossible and approximate averaged methods have to be used. First the pressure can be measured at each plate. Second the voltage difference between the plates can be measured, which gives with the current the total resistance per unit length. This resistance depends mainly on the radially dependent resistivity which varies according to $T_e^{-3/2}$. If by one other measurement the axial peak value of T_e is known, this measurement gives already a first profile information.
For optical analysis a fiber has been installed in any of the cascade plates. Stark broadening of the H–β line gives n_e [23]. A very detailed Voigt deconvolution of Ar II lines has given T_h [24] from the Doppler component of Ar II lines. T_e has again been obtained by the Ar II line/continuum method. In fig. 7 results on n_e are compared with model calculations [25]. It is observed that the measured values are between peak value and radially averaged values as is to be expected. This brings us back to the interrelationship of diagnostics and models. If the latter are formulated in terms of observables a direct comparison can be made. Direct observables are voltage drop, flow velocity and pressure. Stark broadening and Doppler broadening could be calculated from the model, including the lateral integration to permit direct comparison.

In models the boundary conditions are critical factors and also direct information on wall profiles is extremely helpfull. In this respect T_e profile measurements by Pfender et al. by probes very close to the wall should be mentioned. Another measurable quantity is the heat transfer to the wall which can be obtained from the heat transferred to the cooling water at any cascade plate.

Finally we will treat the diagnosis of the expansion of a thermal arc in lower pressure. At the exit of the arc the plasma is sonic with ion fluxes of 10^{20}/s and $n_e/n_o \sim 10\%$. This value is reached in argon, in nitrogen but also in argon/hydrogen and with other admixtures as oxygen, methane and silane. In the arc the dissociation is nearly complete and the ionization will be transferred to atoms with a lower ionization energy, as the plasma is still close to equilibrium. The emanating plasma first accelerates supersonically with velocities approaching 4000 m/s. Then a shock develops followed by a subsonic expansion governed by diffusion.
Several diagnostics have been applied to describe this highly inhomogeneous expansion process: Doppler shift velocity measurements [26], probe measurements [27], spectroscopic measurements [28], UV absorption [29] and Thomson scattering [30]. Electron density in pure argon and argon hydrogen mixtures have been measured with probes in the subsonic expansion by De Graaf et al. [27]. In argon the ion density times the velocity gives (integrated over the surface) the same ion fluence ($\sim 10^{20}$/s) as at the exit of the cascade arc. This is totally changed if hydrogen is admixed; then n_e (and thus the n_i) is reduced by a large factor. This reduction is caused by charge exchange of H^+ with residual

molecules to H_2^+, which recombine dissociatively. If a deposition gas, like silane is injected in an argon ion flow similar processes occur: dissociation by repetitively charge exchange and dissociative recombination. Also in this case a loss of ionization occurs though less severe than in hydrogen admixtures. The absolute line emission method is used by Meeusen et al. [28] to measure the ion composition. As T_e is small (0.2–0.4 eV) excitation from the atomic ground state can be ignored and hence, even at low n_e, highly excited states will be in Saha equilibrium. Therefore, by measuring absolutely highly excited levels of Ar I, H and Si I the ion composition can be calculated from Saha's equation. The result is reported at this conference.

For argon n_0, n_e and T_e have also been measured by Rayleigh and Thomson scattering. Thomson scattering has like LIF the advantage of cross beam and thus local measurement. In the arrangement used by Van de Sanden [30] the scattering plane is perpendicular to the expansion direction. Much attention has been paid to minimize straylight, which in view of the small scattering cross sections is the main problem. Minimum detectable n_e and n_0 are $7.10^{17}/m^3$ and $10^{20}/m^3$ respectively. The resulting n_e, T_e and n_0 [30] are given in fig. 8. The supersonic expansion, shock and subsonic expansion are evident. One observes also that the minimum in T_e occurs before the hydrodynamic shock [30] which could be explained as the consequence of convective current heating. It can be concluded that Thomson scattering is an ideal technique to measure detailed shock phenomena with very good spatial distribution.
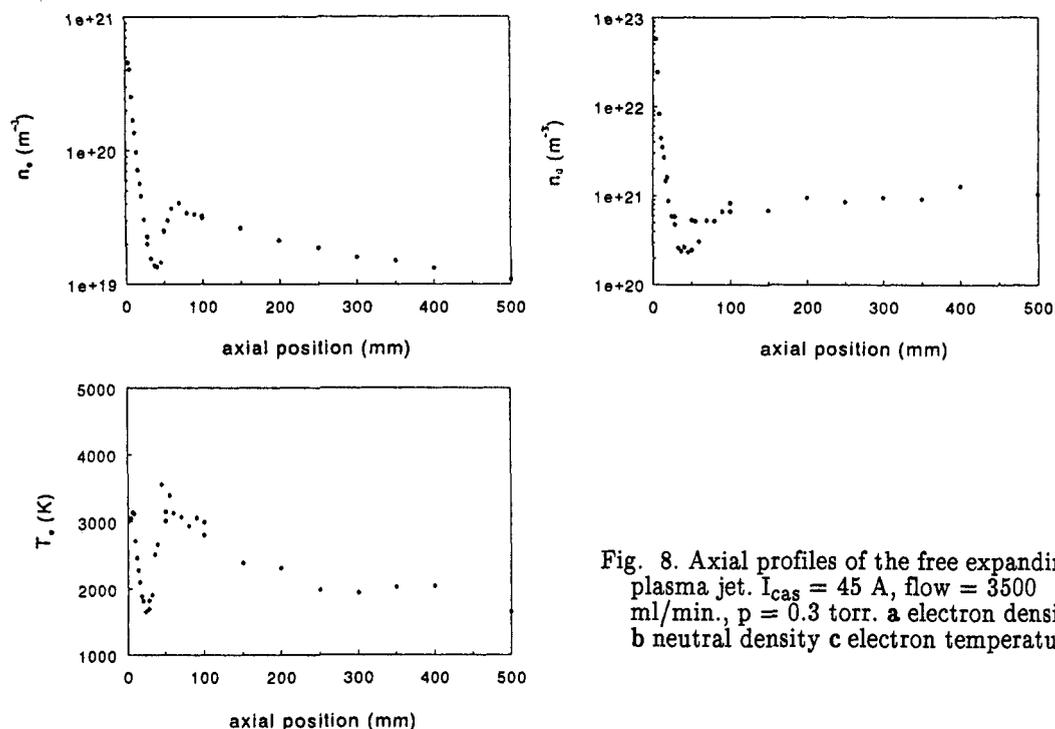

Fig. 8. Axial profiles of the free expanding plasma jet. I_{cas} = 45 A, flow = 3500 ml/min., p = 0.3 torr. a electron density b neutral density c electron temperature

REFERENCES

1. P. Fauchais, J.F. Coudert, M. Vardelle, Diagnostics in thermal plasma processing, Ch. 7 in Plasma diagnostics, Vol. 1, O. Auciello & D.L. Flamm (ed.), Academic Press, Boston (1989)
2. D.C. Schram, I.J.M.M. Raaijmakers, B. van der Sijde, H.J.W. Schenkelaars, P.W.J.M. Bouwmans, Spectrochemica Acta 38B, 1545–1547 (1983)
3. T.L. Eddy, JQSRT 33, 197 (1985)
4. K.P. Nick, J. Richter, V. Helbig, J. Quant. Spectrosc. Radiat. Transfer 32, 1 (1984)
5. R.J. Rosado, An investigation of non–equilibrium effects in thermal argon plasmas, thesis Eindhoven University of Technology (1981)
   C.J. Timmermans, R.J. Rosado, D.C. Schram, Z. Naturforsch. 40A, 810 (1985)

6.   J.A.M. van der Mullen, Physics Report <u>191</u>, 109 (1990)
7.   I.J.M.M. Raaijmakers, P.W.J.M. Boumans, B. van der Sijde, D.C. Schram, Spectrochemica Acta <u>38B</u>, 697 (1983)
8.   V. Helbig, Pure & Appl. Chem. <u>60</u>, 675 (1988)
9.   V. Helbig, K.P. Nick, J. Richter, R.J. Rosado, D.C. Schram, H. Kafrouni, Proc. Vth ESCAMPIG, Dubrovnik, Yugoslavia, 130 (1980)
10. A. Hugenholtz, Microwave interferometer and reflectometer techniques for thermonuclear plasmas, thesis Eindhoven University of Technology; also Rijnhuizen Report 90–192, Nieuwegein, The Netherlands (1990)
11. A.T.M. Wilbers, G.M.W. Kroesen, C.J. Timmermans, D.C. Schram, J. Quant. Spectrosc. Radiat. Transfer <u>45</u>, 1 (1991)
12. C.J. Timmermans, G.M.W. Kroesen, P.M. Vallinga, D.C. Schram, Z. Naturforsch. <u>43A</u>, 806 (1988)
     C.J. Timmermans, An investigation of non–equilibrium effects in thermal plasmas, thesis Eindhoven University of Technology (1984)
13. H.R. Griem, Spectral line broadening by plasmas, Academic Press, New York (1974)
14. P.H.M. Vaessen, J.M.L. van Engelen, J.J. Bleize, J. Quant. radiat. Transfer <u>33</u>, 51 (1985)
15. V. Helbig, Contrib. Plasma Phys. <u>31</u>, 183 (1991) in German
16. H. Haraguchi, T. Hasegewa, M. Abdullah, Pure & Appl. Chem. <u>60</u>, 685 (1988)
17. P.W.J.M. Boumans ed. Inductively Coupled Plasma, Atomic Emission Spectroscopy, Vol. 1, Academic Press, New York (1987)
18. S. Nowak, J.A.M. van der Mullen, B. van der Sijde, D.C. Schram, J. Quant. Spectrosc. Radiat. Transfer <u>41</u>, 177 (1989)
     S. Nowak, J.A.M. van der Mullen and D.C. Schram, Spectrochim. Acta <u>43B</u>, 1235 (1988)
     S. Nowak, J.A.M. van der Mullen, A.C.A.P. van Lammeren and D.C. Schram, Spectrochim. Acta <u>44B</u>, 411 (1989)
19. D.B. Gurevich, I.V. Podmoshenskii, Opt. Spectrosc. <u>18</u>, 319 (1963)
20. F.H.A.G. Fey, W.W. Stoffels, J.A.M. van der Mullen, B. van der Sijde, D.C. Schram, Spectrochim. Acta <u>46B</u>, 885 (1991)
21. E.L. Bydder, G.P. Miller, Spectrochim. Acta <u>44B</u>, 165 (1989)
22. P.H.M. Vaessen, Heat and momentum transfer from an atmospheric argon hydrogen plasma jet to spherical particles, thesis Eindhoven University of Technology (1984)
     D.C. Schram, P.H.M. Vaessen, L.U.E. Konings, G.M.W. Kroesen, Proc. ISPC–7, Eindhoven (1985)
23. G.M.W. Kroesen, C.J. Timmermans, D.C. Schram, Pure & Appl. Chem. <u>60</u>, 795 (1988)
     G.M.W. Kroesen, Plasma Depostion: Investigations on a new approach, thesis Eindhoven University of Technology (1988)
24. J.J. Beulens, M.J. de Graaf, G.M.W. Kroesen, D.C. Schram, Mat. Res. Soc. Symp. Proc. Vol. 190, 311–316 (1991)
25. J.J. Beulens D. Milojevic, D.C. Schram, P.M. Vallinga, A two dimensional non–equilibrium model of cascaded arc plasma flows, to be published in Physics of Fluids
26. G.M.W. Kroesen, D.C. Schram, A.T.M. Wilbers, G.J. Meeusen, Contr. Plasma Phys. <u>31</u>, 27 (1991)
27. M.J. de Graaf, R.P. Dahiya, J.L. Jauberteau, F.J. de Hoog, M.J.F. van de Sande, D.C. Schram, Colloque de Physique, Colloque C5, suppl. 18, Tome 51, 387–392 (1990)
28. G.J. Meeusen, E.A. Ershov–Pavlov, R.F.G. Meulenbroeks, M.C.M. van de Sanden, D.C. Schram, Emission spectroscopy on a supersonically expanding argon/silane plasma, Bochum conference (1991)
29. M. Dudeck, G. Poissant, B.R. Rowe, J.L. Queffelec, M. Morlais, J. Phys. D: Appl. Phys. <u>16</u>, 995 (1983)
30. M.C.M. van de Sanden, J. de Regt, G. Janssen, D.C. Schram, B. van der Sijde, J.A.M. van der Mullen, to be published